CIÊNCIA EXATAS E DA TERRA

Inorganic Pigment Produced from Galvanic Sludge and Kaolinite

Franklin Monteiro Brasil[1], Herley de Souza Silva[2], Genilson Pereira Santana[3]

Abstract

The potentially toxic metals present into galvanic sludge (GS) becomes an environmental problem worldwide. There are several technologies for reducing the high level of the toxic metal, such as ceramic incorporation, calcination, inorganic pigment (IP), etc. The thermical transformation of mixtures composed by clay mineral and GS in IP was evaluated using GS from Manaus Industrial Park and kaolinite chemically obtained by Oxisols that is a spread soil in whole Manaus. Experimentally, 15 samples were prepared to obey the following ratios of GS:kaolinite: 0:1; 1:0; 1:1; 1:2, and 2:1. These samples were ground and calcined at 650, 950 and 1,200 ºC for 9 hours. The calcined samples were characterized by X-ray diffraction (XRD), X-ray fluorescence (XRF), Fourier transformation infrared spectroscopy (FT-IR), three-dimensional CIEL*a*b* projection, metal toxic leaching test, differential scanning calorimeter (DSC), thermogravimetric analysis (TGA), scanning electron microscopy (SEM). Our findings reveal the transformation of GS with chemical structure amorphous in calcite, trevorite, goethite and hematite at 1200 ºC. The leaching reveals the immobilization of toxic metal present in IP. Depending on the proportion of GS/kaolinite can be synthesized an IP with a specific coloring with L* varying from 23.00 to 92.78; a* 2.60 to -0.28; and b* 2.50 to 4.21.

Keywords: Industrial District of Manaus. Potentially Toxic Metal. Environmental Sustainability

Pigmento inorgânico produzido a partir de lodo galvânico e caulinita. Os metais potencialmente tóxicos presentes no lodo galvânico (GS) tornam-se um problema ambiental em todo o mundo. Existem diversas tecnologias para redução do alto teor do metal tóxico, como incorporação cerâmica, calcinação, pigmento inorgânico (IP), etc. A transformação térmica de misturas compostas por argilomineral e GS em IP foi avaliada usando GS do Parque Industrial de Manaus e caulinita obtida quimicamente por Latossolos que é um solo espalhado em todo o Manaus. Experimentalmente, 15 amostras foram preparadas para obedecer as seguintes proporções de GS:caulinita: 0:1; 1:0; 1:1; 1:2 e 2:1. Essas amostras foram moídas e calcinadas a 650, 950 e 1.200 oC por 9 horas. As amostras calcinadas foram caracterizadas por difração de raios-X (DRX), fluorescência de raios-X (FRX), espectroscopia de infravermelho por transformação de Fourier (FT-IR), projeção tridimensional CIEL*a*b*, teste de lixiviação de metais tóxicos,

---

[1] Doutorando Ciência e Tecnologia de Materiais, Universidade Estadual Paulista "Júlio de Mesquita Filho", Guaratinguetá, SP, Brasil e Dpto Química/UFAM, Manaus, AM, Brasil, fmobrasil@gmail.com
[2] Fundação hospital Adriano Jorge - FHAJ, Manaus, AM, Brasil, hsouza@ufam.edu.br
[3] Depo Química, UFAM, Manaus, AM, Brasil, correspondência: gsantana2005@gmail.com

CIÊNCIA EXATAS E DA TERRA

calorímetro diferencial de varredura (DSC), análise termogravimétrica (TGA), microscopia eletrônica de varredura (MEV). Nossos achados revelam a transformação de GS com estrutura química amorfa em calcita, trevorito, goethita e hematita até 1200 °C. A lixiviação revela a imobilização do metal tóxico presente no IP. Dependendo da proporção de GS/caulinita pode ser sintetizado um IP com coloração específica com L* variando de 23,00 a 92,78; a* 2,60 a -0,28; e b* 2,50 a 4,21.

Palavras-chave: Distrito Industrial de Manaus. Metal potencialmente tóxico, Sustentabilidade ambiental

Introduction

The galvanizing process and surface treatment prevent the oxidation of metals and alloys. However, these both consume a large amount of water in its washing steps, as well (Lobato et al., 2015). Therefore, a large amount of GS is produced from physical and chemical treatments of wastewater generated in electroplating manufacturing facilities. GS contains a substantial number of heavy metals, colloidal aluminum hydroxide, aluminum sulfate (used as a flocculating agent), sodium and calcium ions (generated in neutralizing solutions) and water (Pérez-Villarejo et al, 2015). Reminding that in the EU countries, surveys suggest the production of GS about 150,000 t/years (Silva et al, 2005). The most common way to dispose of these wastes is the landfill deposition, though the deposition of GS in landfills is not beneficial for the environment. The literature in chemistry records several technologies such as hydrometallurgy, pyrometallurgy, precipitation, leaching combined with electrochemistry or ultrasound, among others to heavy metal recovery from the polluted environment by GS (Rahimi et al., 2016).

As an alternative, the environmentally sustainable methods of producing new IP by a solid-state reaction from GS of plating processes have presented as an excellent option for environmental sustainability. Depending on GS chemical composition, particularly the nature and content of heavy metal, mainly Ni, Cr, Zn, Fe, and Cd (Vurdova & Lebedev, 2000), the new IP-GS synthesized throughout calcination at 1200 °C produces several colors such as green, red, black, pink, yellow, etc. (Hajjaji et al., 2012). The highly stable, intense tonalities besides compliance with technological and environmental demands proposed by IP-GS is interest for the ceramic industry (Costa et al., 2008).

The techniques used during the synthesis of IP-GS reduce the inevitable production of huge quantities of waste by plating processes. In a complex hydrographical system in which the city of Manaus is located (State of Amazonas-Brazil), plating wastes, containing hazardous contaminants constitute a threat to water, natural resources, and human health due to their drainage and infiltration in the soils. The Manaus Industrial Park has discharged high contents of organic (domestic waste) and inorganic (heavy metal) sewage in Educandos floodplain from Negro River (Pio et al, 2013). This floodplain encompassing an

CIÊNCIA EXATAS E DA TERRA

aquatic system formed by several streams, usually with 1.30-4.00 m, and 0.30-1.6 m along 38 km length (Torrezani et al. 2016). As a result, the riverside inhabitants are affected by all the untreated waste contaminants discharged into the Educandos floodplain (Santana 2015, Santana 2016). The Manaus Industrial Park has over 400 high-throughput state-of-art industrial companies. These companies used high quantities of galvanized products that discharge high plating wastes in the landfill.

As part of researching for generated waste reuse from coating processes from Manaus Industrial Park, it was synthesized a series of new IP using mixtures composed of GS and kaolinite in search of obtaining a competitive product to reduce the environmental impact in the landfills. Generally, it is recommended the TiO_2 in the IP chemical composition. Accordingly, TiO_2 has applied as an opacifying agent in paints, plastics, paper textiles and inks, corrosion-resistant coatings, anti-bacterial agents, water, and air purification, and other (Cava et al., 2002). Alternatively, according to (Alabi & Omojola 2013) when calcined the kaolinite is transformed into mullite exhibiting properties like TiO_2 titanium dioxide.

Kaolinite no oxisol???

For this work, it has been prepared a series of IP using mixtures of kaolinite from Oxisols and GS submitted at different heating temperatures intending to propose an alternative to increasing the life cycle of the solid waste it had output mainly by electro-electronic and motorcycle industries (Manaus Industrial Park).

Experimental part
Sampling of kaolin and GS

IP was prepared from GS resulting from the Cr/Ni plating process and kaolin isolated of Oxisol. The GS is arising from the Manaus Industrial Park, from the Oxisol found in the soil of the city of Manaus (State of Amazonas - Brazil) kaolin was obtained according to the method proposed by (Couceiro & Santana, 1999).

IP preparation

The proportions 0:1, 1:0, 1:1, 1:2 and 2:1 from GS and kaolin were powered by three hours in a ball mill (model). The powered mixtures were calcined at 650, 950 and 1200 °C in a muffle (model EDG 3P-S). The calcination time obeys the following sequence 3, 6 and 9 hours (Klapiszewska et al. 2007, Andreola et al. 2008, Hajjaji et al. 2011, Zhang et al., 2012, Esteves et al. 2013, Hajjaji et al. 2013).

X-ray diffraction of kaolin, GS and IP

X-ray spectrometer was used to determine the chemical composition of kaolin and GS. The morphological structure of all samples was examined by an X-ray diffractometer (Shimadzu, model 6000 LabX) equipped with monochromator graphite and copper tube. For XRD, the samples were triturated and pressed into an aluminum sample holder, and measurements were made from 5 to 70° (2θ) at steps of 0.02° with the counting of 0.6 s step⁻¹.

FT-IR of kaolin, GS and IP

The infrared spectra from kaolin, GS and IP samples were recorded range 4,000 to 400 cm⁻¹ on

CIÊNCIA EXATAS E DA TERRA

a Perkin Elmer spectrophotometer model Spectrum 2000, and 20 scans were performed with a spectral resolution of 4 cm^{-1} according to recommend by (Souza & Santana 2014). Initially, pellets containing nearly 1.0 mg of fraction 50 μm and 100 mg of KBr were dried at 100 °C for 24 hours to remove any humid existing moisture.

DSC-TGA of kaolin and GS

The DSC-TGA thermal analyses were performed in an SDT (model Q600) device attached to a simultaneous thermogravimetric Analyzer (TGA) and Differential Scanning Calorimeter (DSC) that provides simultaneous measurement of weight change (TGA) and true differential heat flow (DSC), in a nitrogenous atmosphere, using a mass sample of about 10 mg, in the temperature interval from 25 to 1400 °C, with a heating rate of 10 °C min^{-1}.

X-ray fluorescence of kaolin and GS

The chemical composition of the kaolin and GS at room temperature and calcined (1200 °C) was obtained by X-ray fluorescence, using a sequential X-ray spectrophotometer Panalytical (Epsilon 3 XL), with a source of Rh.

Inorganic pigment L*a*b* color parameters of IP

The respective coordinates: lightness L* (black-white), a* (green-red) and b* (blue-yellow) of inorganic pigments obtained by GS and kaolin were measured using a spectrophotometer (HunterLab Color-Quest XE) with standard lighting C,

according to the L*a*b* colorimetric method recommended by Commission Internationale de l'Eclairage (CIE)

Leaching test of GS

For determining the leached metal toxic concentration was used the procedure recommended by ASTM. The GS sample was made on a mixture with deionized water in the ratio 1:20 respectively with adjusting of pH between 4.50 and 5.00 under 18 hours of extractions. The extract was filtered through Millipore (0.45 μm) and the heavy metal concentrations determined by ICP-OES (iCAP7600 Duo, Thermo).

Scanning electron microscopy (SEM)

To perform the SEM has used the electron microscope FEI QUANTA 250 in IP samples with deposition of conductive tape, coated with a layer of gold and images recorded under an accelerating voltage of 20 kV, a current of 6.0 x10^{-11} and 5x10^{-7} torr pressure. Furthermore, the mapping of the elements was done by the Energy Dispersive System (EDS) EDAX model.

Result and discussion

The XRF shows the contents of SiO_2, Al_2O_3, and Fe_2O_3 above to natural kaolin composition (Table 1). According to Couceiro & Santana (1999) and Silva et al. (2017), what is expected because of the isomorphic substitution of Al^{3+} by Fe^{3+}. Also, as known, the ideal composition for kaolin, $Al_4(Si_4O_{10})(OH)_8$, is 46.54% SiO_2, 39.50% Al_2O_3, 13.96% H_2O, and as long as in nature, its exact composition is rare (Weaver & Pollard, 1973). The calcination process at 1200 °C

caused a reduction in the SiO_2 content accomplished by an increase of Al_2O_3 content. The present work the SiO_2 reduced 0.88% while Al_2O_3 increased by 1.82%. According to the literature, the formation mullite apart from kaolin occurs generally liberation of silica with the heating at 1200 °C (Weaver & Pollard, 1973).

Table 1- Chemical composition (%) determined by fluorescence of kaolin (Kao) and galvanic sludge (GS) at room temperature (RT) and at 1200 °C

Components	Kao		GS		Ref. 1	Ref. 2
	RT	1,200 °C	RT	1,200 °C		
Al_2O_3	44.692	46.501	0.333	1.152		4.73
SiO_2	52.014	51.136	2.428	6.844		0.17
Fe_2O_3	1.323	1.037	46.621	34.197	0.92	1.57
Cr_2O_3	0.005	0.006	1.202	2.124	50.85	12.8
Na_2O	-	0.003	0.711	11.702	1.30	3.42
NiO	0.001	0.003	12.16	13.628	6.83	12.8
CaO	0.122	0.088	5.483	9.457	30.81	19.5
SO_3	-	-	30.08	16.181		10.6
SiO_2/Al_2O_3	1.16	1.09				

Ref. 1= Garcia-Valles et al. (2007); Ref. 2 = Hajjaji et al. (2012)

The main constituents of the GS were Fe_2O_3, SO_3, CaO, and NiO corresponding to 94.34% other constituents are Al_2O_3, SiO_2, Cr_2O_3, and Na_2O. The major components of the GS were Fe_2O_3, NiO and CaO. The high level of iron and nickel is due to the surface treatment performed in the galvanization process of the material collected in the soil of the Manaus Industrial Park. The XRF shows that the nickel and chromium are the main heavy metal with the potential to cause major environmental problems to the Educandos floodplain (Santana 2016). The high content of CaO is related to using calcium carbonate as an additive in a wastewater treatment plant in the coagulation-flocculation phase for matter in suspension to coagulate and form larger-sized flocs. This facilitates the subsequent decanting process and the calcium sulfate formation (Huyen et al., 2016). The iron content indicates that iron-rich GS is an important source of iron for IP.

Depending on the GS chemical composition the synthesized IP assumes a distinct pigment structure according to the chemical composition reported in the literature (Table 1). For example, (Hajjaji et al. 2012) synthesized three distinct pigment structures: (i) red-wine $Cr–CaSnSiO_5$ and brown $Cr–CaTiSiO_5$; (ii) $Cr-CaTiO_3$; (iii) and $Cr-TiO_2$. On the other hand, (Garcia-Valles et al., 2007)

synthesized the IP of two phases: a spinel phase and a phosphate phase. The calcination caused weight loss of Fe_2O_3 and SO_3 with an increase in other components.

Results from the leaching test in GS shows the metal concentration reduction after calcination at 1,200 °C (Table 2). Particularly, for Cr and Ni, the calcination reduced the toxicity of these heavy metals. The IP produced by calcination at 1,200 °C helps the galvanization reduce its environmental impact. According to Magalhães et al. (2004), the metal degree immobilization is suitable at a temperature above 1,000 °C. It is observed at ≥ 1,000 °C increasing the effectiveness of the metal inertization level.

Table 2 - Heavy metal concentration (mg kg^{-1}) of GS determined by ICP-OES in the leaching test

Heavy metal	RT	1,200 °C
Cu	0.09	0.01
Pb	Nd	Nd
Cd	Nd	Nd
Cr	0.17	0.01
Ag	Nd	Nd
Mn	0.01	0.01
Zn	0.07	0.06
Ni	0.55	0.04
Co	0.001	Nd
Fe	0.04	0.04
Al	Nd	Nd

Nd = Non-detected

As expected, the XRD patterns show only the presence of kaolin and quartz in the kaolin sample (Figure 1). In a reference to the reflections, they indicate that the kaolin (clay mineral) has low crystallinity and/or it is non-ordered. Furthermore, it is possible to observe the relationship between the intensity of the reflections. d_{131} and $d_{(13\bar{1})}$, an important feature observed in XRD, which suggests the existence of monoclinic kaolin. XRD also shows the kaolin transformation according to the increasing temperature. The X-ray patterns points out to the thermal behavior known of kaolin, conveniently divided into four steps:

1. The low-temperature reaction below 400 °C;
2. Intermediate-temperature reactions, mainly between 400 and 650 °C forming metakaolin by dihydroxylation

CIÊNCIA EXATAS E DA TERRA

phenomenon in which occurring a continuous loss of the OH-groups;

3. High-temperature reactions, mainly between 980 and 1,100 °C forming mullite; and

4. Oxidation reaction, mainly between 1,100 and 1,350 °C forming cristobalite.

XRD patterns of GS show the transformation of the goethite during the calcination process in hematite (a-Fe$_2$O$_3$) at 650 °C and trevorite (spinel–NiFe$_2$O$_4$) at 950 °C. Hematite and trevorite coexist at 950-1,200 °C. As expected XRD the calcite only identified at room temperature. Similar

XRD also shows calcite as the main component of the GS (Huyen et al., 2016). The chemical composition GS permits the following transformation (Dunn & Howes, 1996):

1. the first reaction produced a mass loss and oxidation of SO3 to produce sulfate species;

2. the continued formation of sulfate species and an exothermic reaction caused by the conversion of iron sulfide to hematite at 650 °C;

3. the formation of trevorite at 950 °C, and

4. decomposition of calcite at >650 °C.
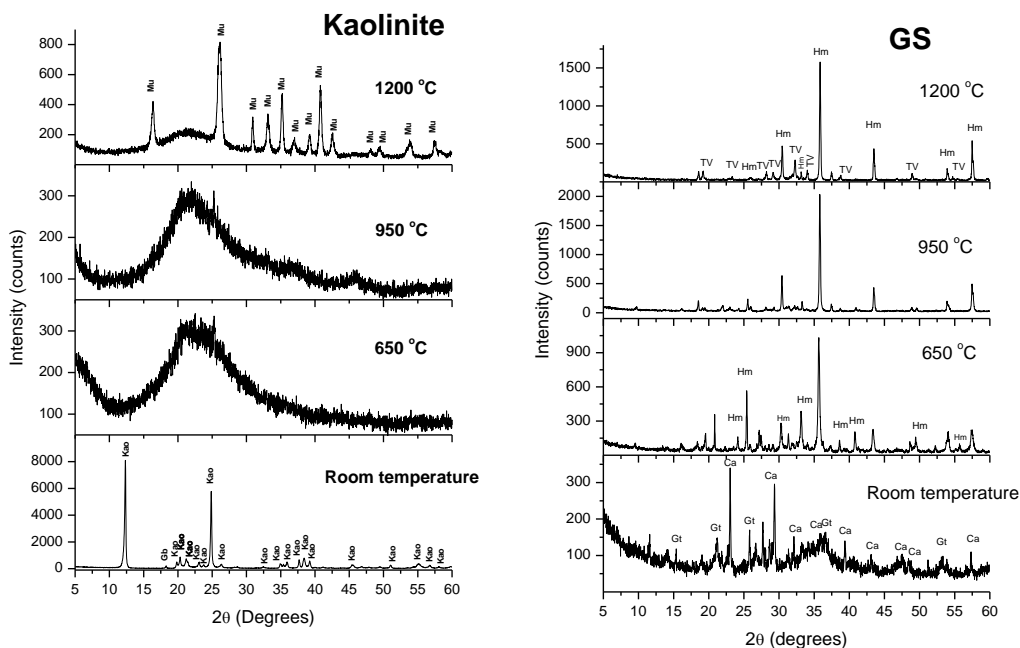
Figure 1 – X-ray patterns of kaolin and GS samples dried from room temperature from 1,200 °C. GT = goethite, Ca = calcite, TV = trevorite, Hm = hematite, Mu = mullite, and Kao = kaolin.

Thus, the weight loss of SO$_3$ and Fe$_2$O$_3$ on calcination of GS causes the formation of trevorite and hematite three compounds that are important IP components. The IP syntheses the SO$_3$ has an important role because it prevents the Cr[6+] formation that is classified as A1 type carcinogens (Calbo et al. 2004).

CIÊNCIA EXATAS E DA TERRA

The DSC-TGA kaolin shows a small weight loss (~7.5%) observed below 100 °C attributed to surface water and around 200 °C (5.0%) typical of adsorbed/intercalated water (Figure 2). The weight loss at around 490 °C (15.0%) evidences the dihydroxylation of the silicate lattice of pure kaolin. DSC shows the following peaks:

1.   around 100 °C relative to surface water endothermic desorption;

2.   around 200 °C indicates loss of intercalated water;

3.   490 °C, an endothermic demonstrating that the intercalation process produced crystal delamination (an effect that facilitates the structure dihydroxylation process) and

4.   around 990 °C there is an exothermic peak relative to the crystallization of the mullite (Wypych & Satyanarayana 2004).
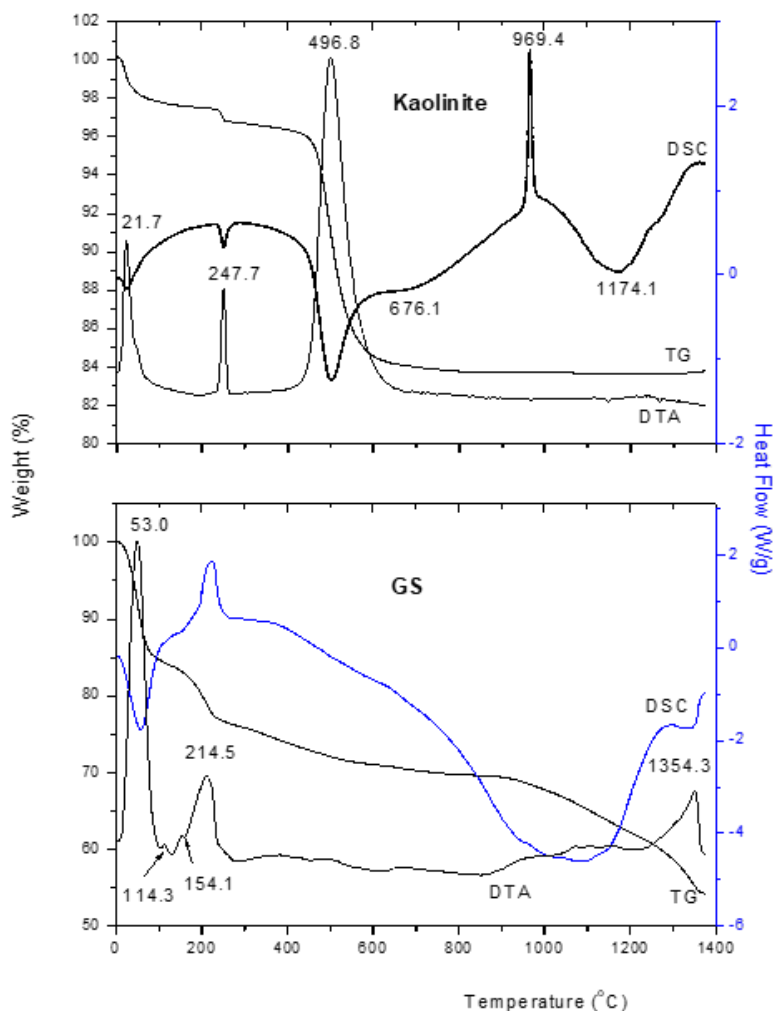
Figure 2 – Thermogravimetry (TG), Differential Scanning Calorimetry (DSC) and Differential Thermal Analysis (DTA) for GS and Kaolin samples.

GS thermal curves show several peaks relative distributed according to i) endothermic peak to

the surface water (75 °C); ii) endothermic peak relative to goethite around 280 °C; iii) a peak relative to

hematite around 650 °C; iv) a peak to trevorite around 950 °C, and v) peaks around 130, 160, 250 (endothermic peak), 1,300 °C (exothermic peak) and 1,350 °C (exothermic peak) relative calcium sulfate.

The FT-IR spectra are again in full agreement with XRD results (Figure 3). The FT-IR spectrum room temperature is remarkably relative to kaolin with bands in 3,669, 3,672, 3,653, 3,631 cm^{-1} corresponding to the vibrations v1, v2, v3 and v4 O-H, respectively. Bands at 1,115 cm^{-1} relatives to Si-O, 1036 and 1009 cm^{-1} on vibration Si-O-Si and 937 and 915 cm^{-1} O-H (Souza & Santana 2014). The kaolin spectrum fired at ≥950 °C with bands at 730 and 560 cm-1 relative to AlO_6, SiO_4 and isolated AlO_4 groups of mullite (Figure 3).
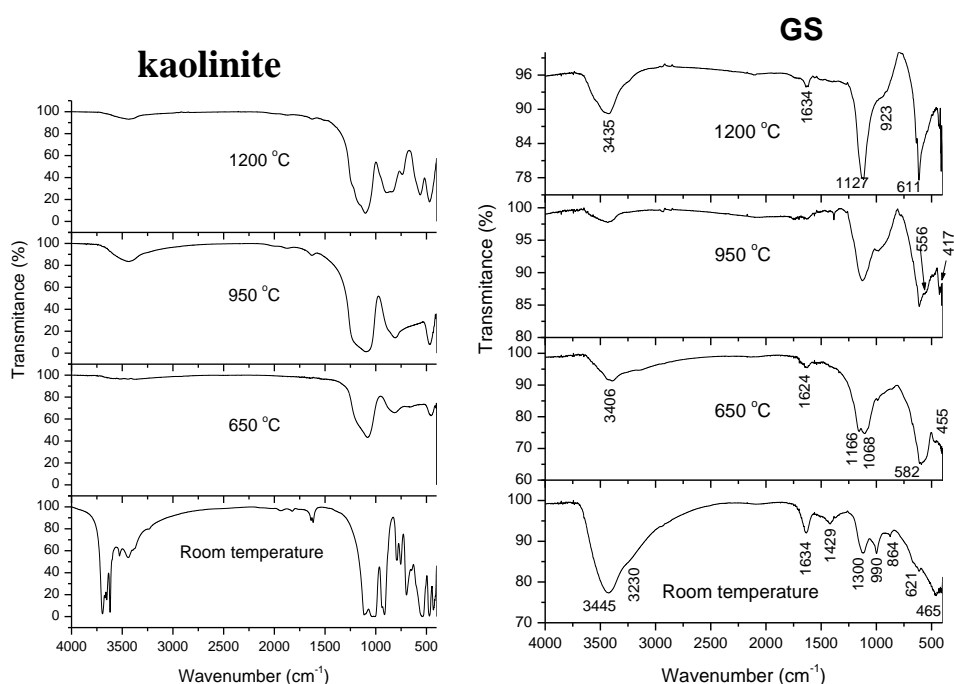
Figure 3 - FT-IR spectra from samples at different temperatures.

The FT-IR for GS at room temperature has the following characteristics typical of goethite: two hydroxyl stretching bands at 3,445 and 3,230 cm^{-1}; one intense hydroxyl bending band at 1,634 cm^{-1}; one hydroxyl translation band at 621 cm^{-1}; one Fe-O vibration at 465 cm^{-1}. The RT spectrum has one stretching vibration at 990 cm^{-1} and asymmetric stretching mode at 1300 cm$_{-1}$ typical of SO_4^{2-}. There also is one stretching vibration at 864 cm^{-1} of calcite. FT-IR at 650 °C presents a large stretching vibrations band (v-H_2O) at 3406 cm^{-1} coupled at a large bending vibrations band (v-H_2O) at 1,624 cm^{-1} attributed to hydrous hematite, 582 and 455 cm^{-1}. In 950 and 1200 °C, the spectra show one 611 cm^{-1} stretching vibrations of tetrahedral groups Fe^{3+}-O^{2-}. These spectra are characterized by v7 and v6 bands near 597 and 417 cm^{-1} indicating the existence of inverse spinel ferrite ferrites. The stretching band at 3,435 cm^{-1} corresponds to nickel ferrite (trevorite).

Inorganic Pigment

The X-ray patterns and FT-IR of IP samples, when heated at 1.200 °C, characterize the transformation of kaolin and the GS (Figure 4). Depending on the GS/kaolin proportion, it's produced a type of IP at 1.200 °C. The proportions 1:1 and 2:1 of GS/kaolin prepare an IP composed by hematite and trevorite, while 1:2 trevorite, hematite, mullite, and calcite. The X-ray diffractions are notably formed by the individual transformation of kaolin and GS into mullite, trevorite, hematite and, calcite
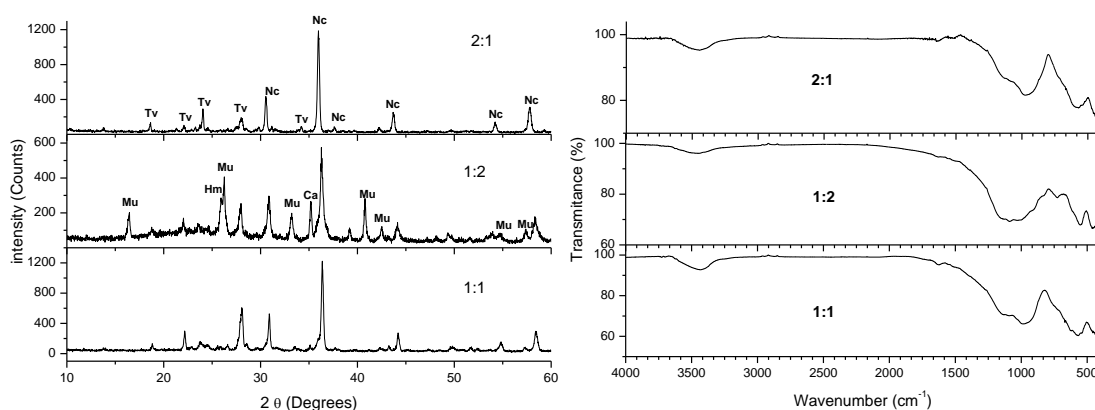

Figure 4– X-ray diffractions and FT-IR of mixture GS and kaolin (1:1) dried from room temperature from 1,200 °C.

Figure 5 shows the SEM for the following proportions of GS/kaolin: 0:1; 1:0; 1:1; 1:2 and 2:1. Undoubtedly, the SEM shows the same crystalline phases detected when heated at 1,200 °C. The ratio of 0:1 phase marks the presence of secondary mullite (Lee et al. 2008). For the ratios of 1:0 and 1:1, it is possible to observe the compound trevorite, represented by small dots on the surface, that are possibly hematites.

In proportion 1:2, the SEM shows the trevorite with low crystallinity and hematite, presenting small whitish spots and mullite without definite shape. In ratio 2:1, the trevorite and hematite it is observed.

Notably, the proportion of kaolin/GS determines the trevorite formation in the IP. It could be related to the amount and transformation of kaolin, as well as the GS chemical composition used to produce IP at 1,200 °C. In principle, the kaolin transformation in mullite is directly influenced by other substances presented during the heating. Li et al. (2009) showed that the presence of salts such as KF, KNO_3, and K_2SO_4 alters the composition and microstructure of mullite. On the other hand, the temperature is an important variable to converter kaolin into mullite. (Kara & Little1996) and Tan (2010), for instance, showed the synthesis of well-developed mullite, at 1.350 °C, with a kaolin mixture in aluminum sulfate. The quote above results supports the findings of Allahverdi et al. (1997), observing the mullite formation is better induced in the presence of sulfate.

Chromatic coordinates of GS-Kaolin calcined at 1,200 °C shows the formation of black and brown pigments (Table 2). These IPs combine the advan-

CIÊNCIA EXATAS E DA TERRA

tageous properties of three different colors according to the Gs and kaolin proportion. In other words, IP produced incorporates chromophores as iron (III), nickel (II) and chromium (III) into the IP crystal lattices.

This work shows that the IP's chemical compositions are typical of pigments used by nearly 25% of the ceramic industry (Calbo et al., 2005). Spinel-system black pigments based on $NiFe_2O_4$ are widely used to decorate a glazed wall and floor tile because they remain stable when mixed with the glaze and when fired at temperatures >1.000 °C (Calbo et al. 2004).

As the main advantage of the IP produced by GS at the Manaus Industrial Park, the mullite's presence it is cited. It's an extender pigment, in whose optical feature, with superior properties, such as gloss, brightness, and yellowness, are quite comparable to titania paint (Ghosh et al. 1990).

Conclusion

The findings show that it is possible to use GS to prepare the IP as an important contribution to the environment sustainability process in the Amazonian region. The feasibility in replacing the oxide titanium by kaolin, a mineral clay practically found in the whole Central Amazon, contributes to immobilizing heavy metals from GS. The results point out the limiting effect of the sulfate to produce trevorite, as well as the isolated transformations of the crystalline phases at 1200 °C. Finally, mullite, trevorite, hematite are crystalline phases formed only between themselves, without external interactions.

0:1

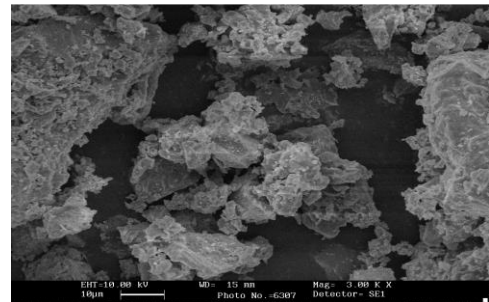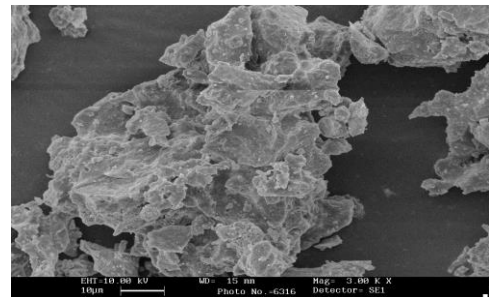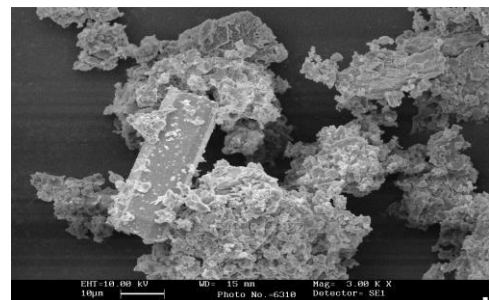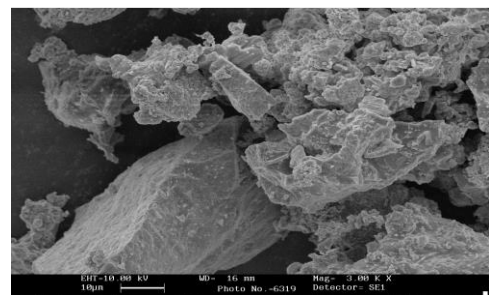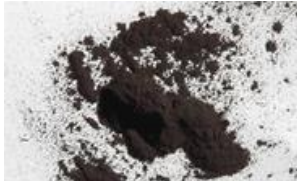**1:1**

2:1

1:2

Figure 5– SEM images of IP prepared at 1,200 °C.

Table 3 - Colorimetric parameters of IP produced from GS and kaolin at 1200 °C

GS: Kaolin ratio	IP	Colorimetric parameters		
		L*	a*	b*
0:1		92.78	-0.28	4.21
1:0		35.89	5.65	6.95
1:1		21.77	3.77	3.64
1:2		43.10	0.57	0.22
2:1		23.00	2.60	2.50

Disclosure

This article is unpublished and is not being considered for any other publication. The author(s) and reviewers did not report any conflicts of interest during their review. Therefore, the journal Scientia Amazônia holds the copyright, has the approval and permission of the authors to publish this article electronically.

Reference

ALABI FM & OMOJOLA M. 2013. Potentials of Nigerian calcined kaolin as paint pigment **Afr J Pure Appl Chem** 7(12):410-417.

ALLAHVERDI M, ALLAIRE C & AFSHAR S. 1997. Effect of $BaSO_4$, CaF_2 and AlF_3 as well as Na_2O on aluminosilicates having a mullite-like composition **J Can Ceram Soc** 66(3): 223–230.

ANDREOLA FL, BARBIERI F, BONDIOLI F, CANNIO M, FERRARI AM & LANCELLOTTI I. 2008. Synthesis of chromium containing pigments from chromium galvanic sludges **J Hazard Mater** 156(1):466-471.

CALBO J, SORLÍ S, LLUSAR M, TENA MA & MONRÓS G. 2004. Minimisation of toxicity in nickel ferrite black pigment Br **Ceram Trans** 103(1): 3–9.

CALBO J., TENA NÁ, MONRÓS G, LLUSAR M, GALINDO R & BADENES JA. 2005. Flux agent effecton nickel ferrite black pigment Am **Ceram Soc Bull** 9201–9209.

CAVAA R J, DISALVOB FJ, BRUSC LE, DUNBARD KR, GORMANE CB, HAILEF SM, INTERRANTEG LV, MUSFELDTH JL, NAVROTSKYI A, NUZZOJ RG, PICKETTK WE, WILKINSONL AP, AHNM C, ALLENN JW, BURNSO PC, CEDERP G, CHIDSEYQ CED, CLEGGR W, CORONADOS E, DAIT H, DEEMU MW, DUNNV BS, GALLIW G, JACOBSONX AJ, KANATZIDISY M, LINZ W, MANTHIRAM A, MRKSICH M, NORRIS DJ, NOZIK AJ, PENG X, RAWN C, ROLISON D, SINGH DJ, TOBY BH, TOLBERT S, WIESNER UB, WOODWARD PM & YAND P. 2002. Future directions in solid state chemistry: report of the NSF-sponsored **workshop Prog Solid State Chem** 30:1-101

COSTA G, RIBEIRO MJ, LABRINCHA JÁ, DONDI M, MATTEUCCI F & CRUCIANI G. 2008. Malayaite ceramic pigments prepared with galvanic sludge **Dyes Pigm** 78(2):157-164.

COUCEIRO PRC & SANTANA GP. 1999. Caulinita em solo da Amazônia: Caracterização e Permutabilidade Acta Amaz 29(2):267-275.

DUNN JG & HOWES VL. 1996. thermochimica acta The oxidation of violarite **Thermochim Acta** 282-283: 305–316.

ESTEVES D, Hajjaji W, SEABRA MP & LABRINCHA JA. 2010. Use of industrial wastes in the formulation of olivine green pigments **J Eur Ceram Soc** 30(15): 3079–3085.

GARCIA-VALLES M., AVLILA G., MARTINEZ SL, TERRADAS R. & NOGUÉS JM. 2007. Heavy metal-rich wastes sequester in mineral phases through a glass – ceramic process **Chemosphere** 68: 1946–1953.

GHOSH S, WARRIER KGK & DAMODARAN AD. 1990. Thermally treated kaolin as an extender pigment **J Mater Sci Lett** 9: 1046–1048

HAJJAJI W, COSTA G, ZANELLI C, RIBEIRO MJ, SEABRA MP & LABRINCHA JÁ. 2012. An overview of using solid wastes for pigment industry **J Eur Ceram Soc** 32(4):753-764.

Hajjaji W, Pullar RC, Zanelli C, Seabra MP, Dondi M & Labrincha JA. 2013. Compositional and chromatic properties of strontium hexaferrite as pigment for ceramic bodies and alternative synthesis from wiredrawing sludge **Dyes Pigm** 96 (3): 659–664.

HAJJAJI W, SEABRA MP & LABRINCHA JA. 2011. Evaluation of metal-ions containing sludges in the preparation of black inorganic pigments **J Hazard Mater** 185(2–3): 619–625.

HUYEN PT, DANG TD, TUNG MT, NGUYEN TTH, GREEN TA & Roy S. 2016. Electrochemical copper recovery from galvanic sludge **Hydrometallurgy** 164: 295–303.

KARA F & Little JA. 1996. Sintering behaviour of precursor mullite powders and resultant microstructures **J Eur Ceram Soc** 16 (6): 627–635.

KLAPISZEWSKA B, KRYSZTAFKIEWICZ A & JESIONOWSKI T. 2007. Pigments precipitated from chromate post-galvanic solutions in emulsion systems **Pol J Chem Technol** 9(1):27-29.

LEE WE, SOUZA GP, MCCONVILLE CJ, TARVORNPANICH T & IQBAL Y. 2008. Mullite formation in clays and clay-derived vitreous ceramics **J Eur Ceram Soc** 28(2):465-471.

Li J, Lin H, Li J & WU J. 2009. Effects of different potassium salts on the formation of

mullite as the only crystal phase in kaolinite **J Eur Ceram Soc** 29: 2929–2936.

LOBATO NCC, VILLEGAS EA & MANSUR MB. 2015. Management of solid wastes from steelmaking and galvanizing processes: A brief review **J Cleaner Prod** 90(1):1-15.

MAGALHÃES JM, SILVA JE, CASTRO FP & LABRINCHA JA. 2004. Role of the mixing conditions and composition of galvanic sludges on the inertization process in clay-based ceramics **J Hazard Mater** 106(2–3): 169–176.

PÉREZ-VILLAREJO L. MARTÍNEZ-MARTÍNEZ S, CARRASCO-HURTADO B, ELICHE-QUESADA D, UREÑA-NIETO C & SÁNCHEZ-SOTO PJ. 2015. Valorization and inertization of galvanic sludge waste in clay bricks **Appl Clay Sci** 105-106:89-99

PIO MCS, SOUZA KS & SANTANA GP. 2013. Capacidade da Lemna aequinoctialis para acumular metais pesados de água contaminada **Acta Amaz** 43(2):203-210.

RAHIMI N, RANDOLPH AP & GRAY EM. 2016. Review of functional titanium oxide. I: TiO_2 and its modifications Prog Solid State Chem 44(3):86-105.

SANTANA GP. 2015. Sediment-distributed metal from the Manaus Industrial District (MID) region (AM, Brazil) J Chem Eng Chem 1(2):55-64.

SANTANA GP. 2016. Heavy metal distribution in the sediment and Hoplosternum littorale from Manaus Industrial district **J Chem Eng Chemistry** 2(2):70-81.

SILVA JE, PAIVA AP & SOARES D. 2005. Solvent extraction applied to the recovery of heavy metals from galvanic sludge **J Hazard Mater** 120(1-3):113-118.

SILVA SS, LAGES AS & SANTANA GP. 2017. Physical and chemical study of lattice kaolinites and their interaction with orthophosphate **An Acad Bras Cienc** 89(2):1391-1401.

SOUZA WB & Santana, PS. 2014. Mineralogy, zinc kinetic adsorption and sequential extraction of contaminated soil in Manaus, Amazon **Cienc Rural** 44(5): 788–793.

TAN H. 2010. Effect of aluminium sulphate on phase formation and morphology development of mullite whiskers Clay Minerals 45(3): 349–353.

TORREZANI L, SARGENTINI JÚNIOR E, OLIVEIRA CAS & SANTANA GP. 2016. Índice de geoacumulação de mercúrio na bacia do igarapé do Educandos (Manaus, Amazonas) J **Chem Eng Chem** 2(3):161-170.

VURDOVA NG & LEBEDEV DN. 2000. Environment protection – Promising approaches to recycling effluent residues from galvanizing operations **Metallurgist** 44(9):24-25.

WEAVER CE. & POLLARD LD. 1973. The chemistry of clay minerals. Amsterdam: Elsevier.

WYPYCH F & SATYANARANYANA KG. 2004. Clay surfaces - Fundamentals and appications. Amsterdam: Elsevier.

ZHANG L, ZHENBANG P, CHAO Y, XIKE T & SUXIN Z. 2012. Synthesis of Chromium-Doped Malayaite Pigments from Wastewater Containing Low Chromium (VI) J **Air Waste Manag Assoc** 2247.